

Upgrade of the helically symmetric experiment Thomson scattering diagnostic suite

Cite as: Rev. Sci. Instrum. **93**, 093518 (2022); <https://doi.org/10.1063/5.0101879>

Submitted: 03 June 2022 • Accepted: 17 August 2022 • Published Online: 26 September 2022

 W. R. Goodman, E. R. Scott, Z. Keith, et al.

COLLECTIONS

Paper published as part of the special topic on [Proceedings of the 24th Topical Conference on High-Temperature Plasma Diagnostics](#)



View Online



Export Citation



CrossMark

ARTICLES YOU MAY BE INTERESTED IN

[A diagnostic to measure neutral-atom density in fusion-research plasmas](#)



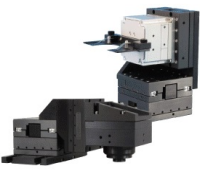
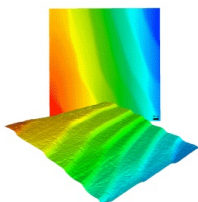
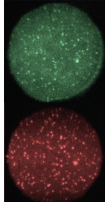
Review of Scientific Instruments **93**, 093519 (2022); <https://doi.org/10.1063/5.0101683>

[Measurement of electromagnetic waves from runaway electrons](#)

Review of Scientific Instruments **93**, 093516 (2022); <https://doi.org/10.1063/5.0101650>

[Quantifying electron temperature distributions from time-integrated x-ray emission spectra](#)

Review of Scientific Instruments **93**, 093517 (2022); <https://doi.org/10.1063/5.0101571>

 MAD CITY LABS INC. www.madcitylabs.com	<p>Nanopositioning Systems</p> 	<p>Modular Motion Control</p> 	<p>AFM and NSOM Instruments</p> 	<p>Single Molecule Microscopes</p> 
---	--	--	---	--

Upgrade of the helically symmetric experiment Thomson scattering diagnostic suite

Cite as: Rev. Sci. Instrum. 93, 093518 (2022); doi: 10.1063/5.0101879

Submitted: 3 June 2022 • Accepted: 17 August 2022 •

Published Online: 26 September 2022



W. R. Goodman,^{a)} E. R. Scott, Z. Keith, L. Singh, and D. T. Anderson

AFFILIATIONS

HSX Plasma Laboratory, University of Wisconsin, Madison, Wisconsin 53703, USA

Note: This paper is part of the Special Topic on Proceedings of the 24th Topical Conference on High-Temperature Plasma Diagnostics.

^{a)}Author to whom correspondence should be addressed: wgoodman2@wisc.edu

ABSTRACT

The Helically Symmetric eXperiment (HSX) Thomson Scattering (TS) diagnostic is being upgraded to decrease uncertainty in electron temperature and density measurements. Upgrades to the HSX TS diagnostic will consist of a novel redesign of polychromator electronics and digitization of the TS output signal. Here, we also present a study of the benefits of an additional spectral channel that will sample the red-shifted band of the scattered spectrum. To maximize system bandwidth (BW) and gain, while minimizing noise, the existing low-BW polychromator electronics on HSX will be replaced by high-BW, high gain circuitry designed in-house.

Published under an exclusive license by AIP Publishing. <https://doi.org/10.1063/5.0101879>

I. INTRODUCTION

Thomson scattering is a workhorse diagnostic in all major fusion plasma research experiments.^{1–3} Although the Helically Symmetric eXperiment (HSX) Thomson Scattering (TS) diagnostic, in its present state, has been operational since 2004,⁴ advances in the available technology and analytic techniques have motivated upgrades to the existing diagnostic suite. Newly designed polychromator electronics have been engineered to reduce measurement uncertainty by both improving the fidelity of measured signals and allowing for a more robust method of modeling the expected signal intensity. Charge integrating digitizers (QDCs) lack the ability to provide time-resolved signals and, therefore, information on abnormalities that may occur during the QDC integration time. HSX is replacing existing QDCs with 1.25 GS/s time-resolved digitizers that will allow for the implementation of curve fitting and more accurate analysis routines in post-processing. Also presented in this work is a study of the benefits of adding a long-wavelength, or long- λ , spectral channel to low-temperature TS spatial channels, $T_e < 200$ eV, such as those at the plasma edge.

II. EXISTING SYSTEM

HSX is currently equipped with a ten-channel TS system that measures T_e and n_e along a 20 cm lower half-plane radius. A

commercial Q-switched Nd:YAG laser provides the probe pulse of 1 J with a 10 ns full width at half maximum (FWHM) at the fundamental 1064 nm wavelength. The laser is housed in a controlled environment located within the main HSX lab. Three mirrors guide the laser beam to the entrance of the HSX vessel. To minimize stray light, the beam enters the vessel via a custom Brewster window and traverses an entrance tube with stray light mitigation baffles. Scattered radiation from the plasma beam interaction is collected by a pair of BK7 and SF1 glass doublet optics and images the light onto ten radial fibers with a numerical aperture (NA) of 0.23. Each fiber bundle is 7 m long and couples the collected light to ten General Atomics (GA) GAPD-1064-4-1K polychromators.^{5,6} Within the GA polychromators, EG&G C30956E Si avalanche photodiodes (APDs) convert the scattered light signal into an electrical current, which is then processed into an output voltage that is sampled by LeCroy Model 2250 QDC. Since the DC component of the plasma background radiation is undesirable when computing TS profiles, an AC-coupled output that removes the extraneous DC signal is often implemented. The GA polychromator electronics perform AC-coupling by use of a 100 ns delay line technique that subtracts the delayed signal from the non-delayed signal, approximately removing the background DC signal.

Initially designed as identical polychromators with four dedicated spectral channels each, the GA polychromators have been modified from their original specifications to allow the five core

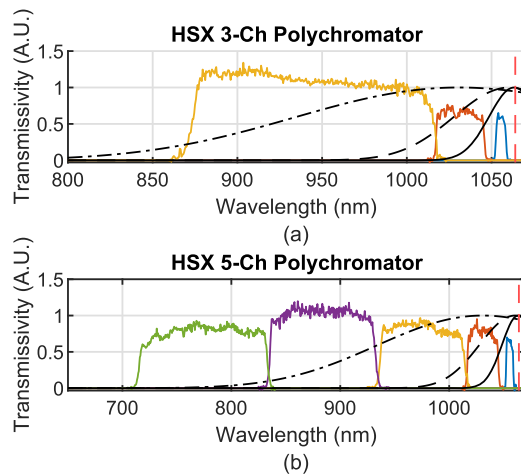


FIG. 1. Transmission functions for the existing (a) three-channel and (b) five-channel HSX polychromators. Included on the plots are the input laser line, shown as a dashed red line, as well as the normalized 90° scattering spectra for 50, 250, and 2500 eV, depicted by the black solid, dashed, and dashed-dotted lines, respectively.

spatial channels to have five spectral channels each, whereas the five edge spatial channels only have three spectral channels each, as shown in Fig. 1. To mitigate low signal strength, passive component changes have been made to polychromator electronics with the goal of increasing the system gain. Data shot from the existing HSX TS system, Fig. 2, have been collected in a Raman scattering configuration with a 4 GS/s oscilloscope. Referring to Fig. 2, an unintended consequence of the modifications to the GA polychromator electronics has been the reduction of system bandwidth, which increases the fall time of the scattered signal output to ~ 400 ns, much greater than the 100 ns delay line time. Only 100 ns of the signal is digitized by the QDC, leaving nearly 80% of the scattered signal unmeasured

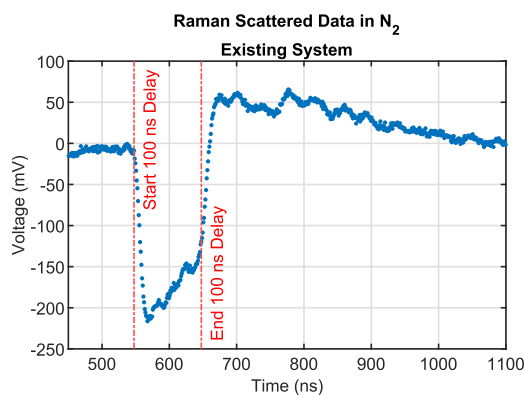


FIG. 2. Raman scattered data on the polychromator AC output channel digitized by a 4 GS/s oscilloscope. The steep transition from negative to positive at ~ 650 ns is caused by the internal 100 ns delay line circuit in the polychromator electronics. Ideally, all scattered signal should be contained within 100 ns as to not be affected by the internal delay line.

and discarded. Recent testing has shown that while the system gain was increased from 90 to 125 dB Ω , this was for low-frequency operation. When accounting for a 10 ns Gaussian pulse and its corresponding high-frequency components, the realized gain is only 74 dB Ω . Due to low signal levels associated with the existing HSX TS system, the aforementioned modifications were necessary. Advances in consumer-grade ICs have allowed for advanced TS electronics designs for diagnostic upgrades.

III. TIME-RESOLVED DIGITIZATION TO DECREASE UNCERTAINTY

A simple method to decrease measurement uncertainty in TS signals is to replace QDCs with time-resolved analog-to-digital converters (ADCs). There are two benefits realized with a time-resolved measurement of the TS signal. First, a time-resolved measurement of scattered radiation allows the experimentalist to validate the collected data and discriminate signals that have been corrupted, e.g., by acute external noise or stray light. Additionally, switching from QDCs to ADCs allows the use of curve fitting techniques that can reduce or eliminate unwanted and spurious contributions to the measured signal.^{7–9} For the HSX TS upgrade, existing LeCroy QDCs are being replaced with a 40-channel, 1.25 GS/s, 8-bit, VT861 digitizer chassis manufactured by LYRtech. To accommodate the switch from QDCs to ADCs, the HSX team is developing new analysis software that utilizes curve fitting techniques to analyze TS measurements. Switching from QDCs to high-speed digitizing ADCs necessitates an upgrade of the existing polychromator electronics, which is discussed in Sec. IV.

IV. POLYCHROMATOR ELECTRONICS UPGRADE

A. Design and simulation

The primary goal of the HSX TS polychromator electronics redesign is to accurately measure and sample the scattered radiation pulse, while introducing little to no curve shaping in the process. For curve fitting routines, the easiest way to decrease uncertainty from the curve fit is to minimize the number of free parameters that are used in the fitting routine. A single-pulse Gaussian can be fit with three free parameters, possibly even one with a well-characterized TS system, whereas systems with excess pulse shaping require four or more fitting parameters to account for the long fall delay time. To capture the primary frequency components of the measured Gaussian pulse,¹⁰ a system must have a minimum upper -3 dB point as defined by Eq. (1),

$$-3 \text{ dB}_{\text{upper}} \approx \frac{0.44}{T}, \quad (1)$$

where T is the FWHM of the Gaussian pulse. Therefore, for the HSX 10 ns FWHM pulse, the upper -3 dB point design requirement should be a minimum of 44 MHz.

With the minimum system bandwidth constraint defined, secondary goals in the design of new sensing electronics, in order of importance, are as follows: minimization of system noise, maximization of electronics gain, implementation of digital gain control, minimal alteration to the existing TS setup, and simplification of calibration procedures. To accomplish the outlined design goals,

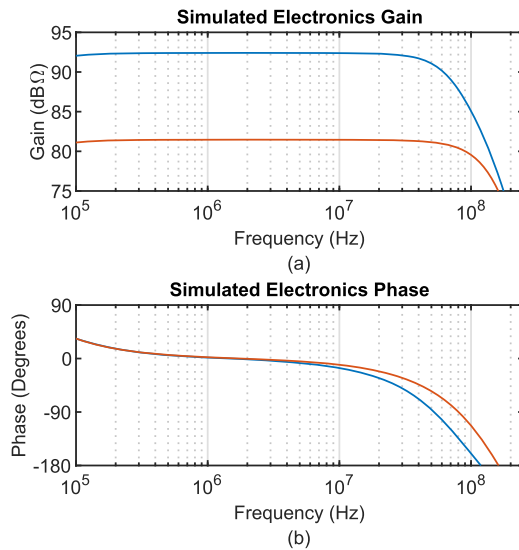


FIG. 3. AC analysis (a) gain and (b) phase frequency response results of designed TS electronics performed in TINA-TI. The blue curve corresponds to the high gain configuration and the orange curve corresponds to the low gain configuration. Simulated upper -3 dB points are 67 and 118 MHz for the high and low gain configurations, respectively.

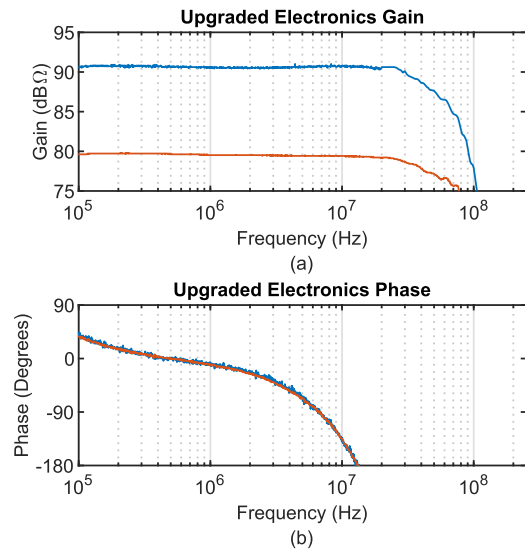


FIG. 4. Measured (a) gain and (b) phase frequency response of the designed TS polychromator electronics. The blue curve corresponds to the high gain configuration and the orange curve corresponds to low gain configuration. Measured upper -3 dB points are 45 and 64 MHz for the high and low gain configurations, respectively.

a Texas Instruments (TI) OPA857 discrete transimpedance amplifier (TIA) was selected for the initial preamplifier stage in a signal chain similar to Fig. 39 in the OPA857 datasheet.¹¹ Device highlights of the OPA857 are ultralow noise, 100 MHz operation, two user selectable gain configurations, and an integrated voltage-to-current converter. The OPA857 voltage-to-current converter allows for frequency response characterization of the circuit without the need for an APD, so the entire system frequency response can be analyzed with standard lab equipment. For even more gain, a TI THS4541 650 MHz gain-bandwidth (GBW) operational op-amp was chosen for the output amplifier stage. On TS AC channels, the use of delay lines to remove the DC component of the Thomson signal has the nonideal effect of doubling high-frequency noise. Therefore, on our newly designed electronics, AC-coupling is performed by the use of a matched $50\ \Omega$ pulse transformer with a high-pass frequency cutoff of 300 kHz. Figure 3 shows the frequency response characteristics of the designed circuit as simulated in Toolkit for Interactive Network Analysis-TI (TINA-TI), a TI supplied simulation program with integrated circuit emphasis (SPICE) program.

B. Electronics test results

As described in Sec. IV A, the upgraded TS printed circuit board (PCB) was designed, laid out, and populated in-house. To validate the functionality of the newly designed PCB, we performed frequency characterization and compared the measured data to results from simulation. With the ability to evaluate the circuit via the integrated current-to-voltage converter, input stimulus was driven by an Agilent arbitrary waveform generator and an Agilent 1 GHz oscilloscope was used to measure the output response relative to the input stimulus. A script was written in MATLAB that automatically swept the function generator output frequency

and obtained data from the oscilloscope. The measured frequency response data of the upgraded electronics are presented in Fig. 4, whereas the measured and simulated results are compared in Table I. Nominal discrepancies between simulated and measured values of maximum gain can be accounted for by nonideal discrete components and board layout. The reduction in measured system bandwidth (BW) relative to the simulated BW is thought to be due to excess input and parasitic capacitances on the PCB. More testing and component optimization will take place before the upgraded TS electronics are installed into the existing TS system. Figure 5 shows the upgraded TS electronics output corresponding to a single Raman scattered pulse in an N_2 environment. From 450 to 500 ns, before the arrival of the laser pulse, nominal system noise of 10 mV_{pk-pk} is measured. Also shown in Fig. 5 is how spurious fluctuations, from plasma noise or stray light, can be measured and systematically removed for analysis by the use of curve fitting routines. The solid orange curve in Fig. 5 shows the results of a simple Gaussian pulse curve fitting routine applied to the measured signal. It is clear that high-bandwidth measurements coupled with curve fitting techniques allow for the removal of most spurious signal contributions and their effects on TS analysis.

TABLE I. Comparison of simulated and measured HSX TS upgrade polychromator electronics results.

Gain mode	Gain (sim) (dB Ω)	Gain (meas) (dB Ω)	BW (sim) (MHz)	BW (meas) (MHz)
High	92.4	90.9	67	45
Low	81.5	79.7	118	64

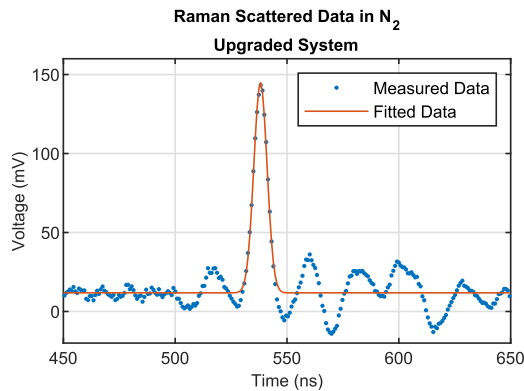


FIG. 5. Measured response of the upgraded TS electronics, low gain configuration, to a Raman scattered pulse (blue curve). Overlaid is an example of a Gaussian fit to the scattered data (orange curve). The HSX vessel was filled to a pressure of 40 Torr N_2 for this measurement. 10 mV_{pk-pk} system noise can be seen in the 450–500 ns range.

V. STUDY OF LONG- λ SPECTRAL CHANNEL EFFECTS ON MEASUREMENT UNCERTAINTY

Generally, for systems that utilize fundamental 1064 nm probe beams, only the shorter blue-shifted lobe of the scattered radiation is collected and analyzed. While some experiments have implemented spectral filters that measure wavelengths longer than the laser line radiation,¹² conventional Si APDs that are used have diminishing responsivity at these wavelengths and are generally only good to signify the possibility of a non-Maxwellian thermal distribution. An alternate approach that we investigate here is the use of a long- λ sensitive InGaAs APD to measure the red-shifted scattered radiation spectrum.

In order to evaluate the possible benefits of adding a long- λ spectral channel to our existing polychromators, a Monte Carlo (MC) analysis was performed on synthetic TS data. For this analysis, a readily available off-the-shelf Excelitas C30662 InGaAs APD was selected for modeling purposes. As we currently do not have spectral calibration data for wavelengths longer than the laser line radiation, the optics transmission is assumed to be constant for the range $1060 < \lambda < 1550$ nm. To maintain signal levels on existing spectral channels, the long- λ spectral channel will be installed subsequent to the existing polychromator channels. Data for a Thorlabs long-pass spectral filter that allows $\lambda > 1070$ nm are used. The final modeled parameter is that the APD gain is increased to $M = 40$, a best case figure for the selected component. With the prior assumptions and parameters, the modeled transmission function for the existing HSX polychromators with an additional long- λ channel is shown in Fig. 6.

Synthetic data for the Monte Carlo analysis was derived by convolving the modeled instrument functions corresponding to each spectral channel with scattered power spectrum data obtained from implementing the often used Matoba model¹³ of Thomson scattered power. Figure 7 shows the normalized, unperturbed intensity model as a function of T_e used for the MC analysis. Simulation consisted of 10 000 ratio evaluations performed at each value of T_e , from 1 to 250 eV, with a randomly distributed perturbation factor of 0.90–1.10

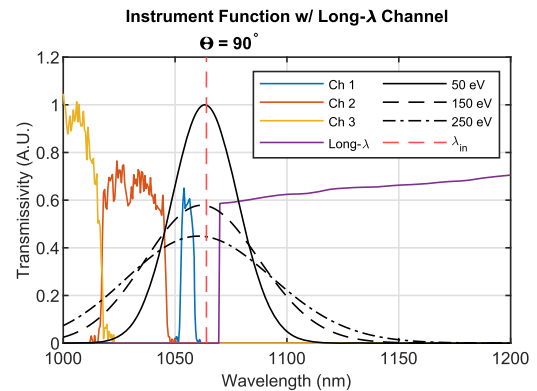


FIG. 6. Instrument function of the existing HSX polychromator system with the modeled long- λ spectral channel being studied.

applied to each data point. Using the same ratio-evaluation χ^2 minimization routine to solve for T_e that will be used for plasma analysis, the standard deviation of perturbed data with and without a long- λ channel were simulated and compared for all five edge channels.

The results of this analysis are shown in Fig. 8. It is shown in Fig. 8 that, assuming optimum conditions, the addition of a long- λ spectral channel will decrease measurement uncertainty by $\sim 25\%$, without compromising the signal strength of existing spectral channels. Interestingly, in Fig. 8, the measurement uncertainty of the long- λ spectral channel increases around 200 eV, $\frac{\sigma_{long\lambda}}{\sigma_{current}} > 1$. Referring to Fig. 7, the cause of this increased uncertainty is due to the relative intensities of multiple spectral channels converging around a common value, ~ 175 eV. When the modeled spectral intensity ratios converge around a common value, the χ^2 minimization routine is much more sensitive to perturbations in the data, which can increase $\sigma_{long\lambda} > \sigma_{current}$, as is the case in this study. Changes to the spectral transmission instrument function, such as further optimized filter functions, can be used to mitigate this increase in uncertainty.

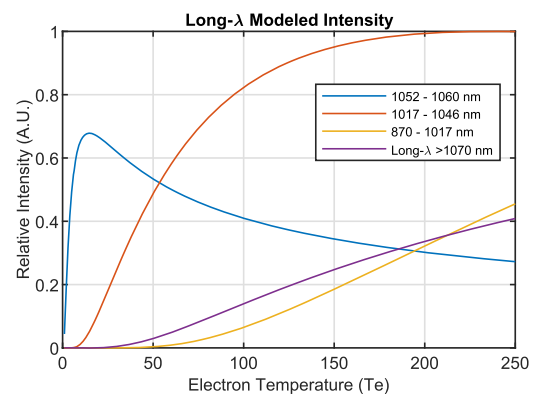


FIG. 7. Normalized product of spectral transmission instrument function convolved with modeled scattered power spectrum.

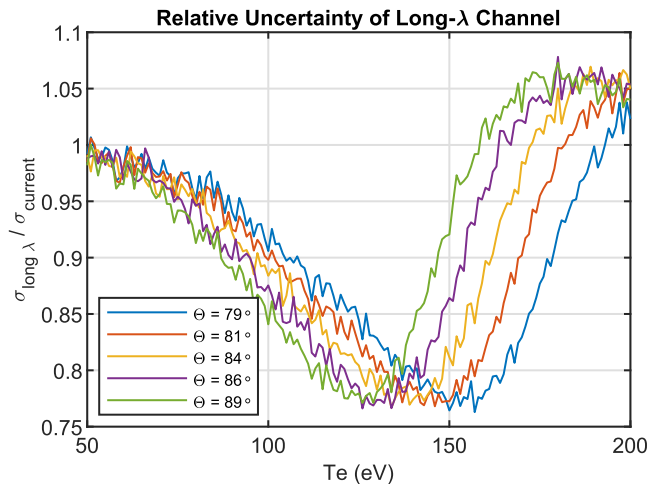


FIG. 8. Results from MC simulations of the effects of adding a long- λ spectral channel. Each curve corresponds to a different edge spatial channel, as determined by the scattering angle Θ . For each edge spatial channel, the standard deviation of the long- λ spectral channel normalized by the standard deviation of the existing polychromator setup as a function of T_e is plotted. For most of the displayed range of T_e , measurement uncertainty is decreased when the long- λ spectral channel is present.

VI. SUMMARY

The HSX TS system is currently being upgraded to improve the fidelity of TS measurements. Transition from existing QDCs to high-speed, time-resolved ADCs will provide greater insight into the quality of collected TS data and decrease measurement uncertainty. Design and initial testing has been performed on custom high-BW polychromator electronics and the benefits of these higher-BW electronics have been demonstrated. The tests have also shown the effect that parasitic capacitances from PCB layout can have on system bandwidth. The initial study of the inclusion of a long- λ spectral channel demonstrates the reduction of measurement uncertainty for a select range (~ 50 – 150 eV) of low plasma temperatures.

ACKNOWLEDGMENTS

This work was supported by U.S. DOE Award No. DE-FG02-93ER54222.

AUTHOR DECLARATIONS

Conflict of Interest

The authors have no conflicts to disclose.

Author Contributions

W. R. Goodman: Data curation (equal); Formal analysis (equal); Investigation (equal); Methodology (equal); Writing – original draft (equal); Writing – review & editing (equal). **E. R. Scott:** Conceptualization (equal); Supervision (equal); Validation (equal); Writing – review & editing (equal). **Z. Keith:** Data curation (equal); Software (equal); Validation (equal); Writing – review & editing (equal). **L. Singh:** Conceptualization (equal); Writing – review & editing (equal). **D. T. Anderson:** Funding acquisition (lead); Supervision (lead); Writing – review & editing (supporting).

DATA AVAILABILITY

The data that support the findings of this study are available from the corresponding author upon reasonable request.

REFERENCES

- ¹I. Hutchinson, *Principles of Plasma Diagnostics*, 2nd ed. (Cambridge University Press, Cambridge, 2005).
- ²D. H. Froula *et al.*, *Plasma Scattering of Electromagnetic Radiation*, 2nd ed. (Academic Press, 2011).
- ³H. Hartfuß, *Fusion Plasma Diagnostics with Mm-Waves*, 1st ed. (Wiley-VCH, Weinheim, Germany, 2013).
- ⁴K. Zhai *et al.*, “Performance of the Thomson scattering diagnostic on helical symmetry experiment,” *Rev. Sci. Instrum.* **75**, 3900 (2004).
- ⁵C. L. Hsieh *et al.*, “Silicon avalanche photodiode detector circuit for Nd:YAG laser scattering,” *Rev. Sci. Instrum.* **61**, 2855 (1990).
- ⁶T. N. Carlstrom *et al.*, “Design and operation of the multipulse Thomson scattering diagnostic on DIII-D (invited),” *Rev. Sci. Instrum.* **63**, 4901 (1992).
- ⁷R. O’Connell *et al.*, “Optimizing a Thomson scattering diagnostic for fast dynamics and high background,” *Rev. Sci. Instrum.* **79**, 10E735 (2008).
- ⁸J. H. Lee *et al.*, “Research of fast DAQ system in KSTAR Thomson scattering diagnostic,” *J. Instrum.* **12**, C12035 (2017).
- ⁹K. C. Hammond *et al.*, “Initial operation and data processing on a system for real-time evaluation of Thomson scattering signals on the large helical device,” *Rev. Sci. Instrum.* **92**, 063523 (2021).
- ¹⁰M. I. Skolnik, *Radar Handbook*, 2nd ed. (McGraw-Hill, New York, 1990).
- ¹¹OPA857 Ultralow-Noise, Wideband, Selectable-Feedback Resistance Transimpedance Amplifier, Texas Instruments, rev. D, 2016.
- ¹²S. Z. Kubala *et al.*, “Upgrades to improve the usability, reliability, and spectral range of the MST Thomson scattering diagnostic,” *Rev. Sci. Instrum.* **87**, 11E547 (2016).
- ¹³T. Matoba, “Analytical approximations in the theory of relativistic Thomson scattering for high temperature fusion plasma,” *Jpn. J. Appl. Phys.* **18**, 1127 (1979).